

Nonlinear Analysis of Arch hollow box RC Beams with openings in different locations

*Yasar Ameer Ali Mubarak , Alaa Hussien Ali

Al-mustaqbal University College-hillah-iraq

* E-mail of the corresponding author: yessarameer@mustaqbal-college.edu.iq

Abstract

This study is devoted to investigate the behavior and performance of arch reinforced concrete (R.C.) beams with openings in different locations along the beam at degrees of 15°, 30°, 45°, 67.5° and 90°. For the analysis, the ANSYS V.16.0 software is used. The ordinary R.C. was modeled by 8-noded isoparametric brick elements, while the steel reinforcing bars were modeled as axial members (bar elements) connecting opposite nodes in the brick elements with full interaction assumption. The CFRP strips were modeled by shell elements. Results show that the ultimate capacity of the beams decreased when the location of the opening changed from 15° to 45° and return to increase when the location of the opening changed from 45° to 90°.

Keywords: reinforced concrete beam, arch beam, opening.

Introduction

The main aim of an arch is to enhance the load carrying capacity, which may come from the stiffening behavior due to membrane action (**Zainul-Abideen, 2010**). According to **Nimmim (1993)**, the design of arch R.C. bridge girders, hollow sections are often adopted in order to:

1. Reduce the weight which affects especially the cost of transport, handling and erection for precast cross sections and also reduce the transport weight for other members of construction.
2. Substantial reduction of material quantities, the materials required are usually much less than those needed for other conventional systems.
3. Hollow box cross section is used for concealed mechanical or electrical runs and also to provide partial flange rotational restraints.

So in order to use the hollow cross section arch beam to conceal electrical or mechanical runs it is necessary to install transvers openings through the profile of the beam in order to pass these runs. And the transvers openings may also be used to pass some primary services like telephone, sewage, and computer networks. In recent building construction, a web of ducts and pipes are needed to accommodate primary services like sewage, telephone, electricity, water supply, computer network, and air-conditioning. Usually, these ducts and pipes are always installed under the beam soffit and a suspended ceiling is used to cover these ducts and pipes for aesthetic reasons, thus a dead space will be created. But the dead space is reduced when these ducts and pipes pass through transverse openings in the web of the beam and result in a more compact design. This saving that achieved may not be important for small buildings, but any saving in the height of a story for multistory buildings, multiplied by the number of stories can represent a fundamental saving in total length, height of electrical ducts and plumbing risers, air-conditioning , partition surfaces and walls, and; therefore, overall load on foundations (**Mansur, 2006**).

It is clear that including of openings in beams changes the beam simple behavior to a more complicated one. Due to sudden changes in sectional configuration, high stress concentration subjected to the corners of opening that may lead to unacceptable cracking from durability and aesthetic viewpoints. The reduction in the beam stiffness may also lead to rise in the excessive deflection under service load and also lead to a major redistribution of moments and internal forces in a continuous beam. Such a beam is highly effected by its strength and serviceability, so a special reinforcement is needed in sufficient quantity in order to resist the reduction in strength with proper detailing, (**Mansur, 2006**).

Different sizes and shapes of openings may be used, and the openings are positioned mainly near the supports where the shear controls. In spite of many shapes are possible, rectangular and circular shapes are the most used ones. Rectangular openings are mostly used for air conditioning ducts, which are mostly rectangular, while circular openings are used for sewage and other service pipes.

1-Finite Element Representation of the R. C. Beam:

The element types for this model are shown in Table (1). The **CONCRETE65** element was used to model the concrete. This element has eight nodes with three degrees of freedom at each node translation in the nodal x, y and z directions. This element is capable of plastic deformation, cracking in three orthogonal directions and crushing. Link 8 was used to represent the flexural reinforcement while **SOLID45** elements were used to model the plate loading and supporting, **ANSYS 16.0 (2015)**.

Table(1): Element types for working model.

Material type	ANSYS element
Concrete	SOLID 65
Flexural Reinforcement and stirrups	LINK 8
Plate loading and supporting	SOLID45

1-1 Concrete Brick Element:

The 8-node isoperimetric linear element (**CONCRETE65**) in the **ANSYS 16.0** program, used in the study, is shown in fig (1). Each node, of the eight corner nodes, has three degrees of freedom u, v, and w in the X, Y and Z directions respectively.

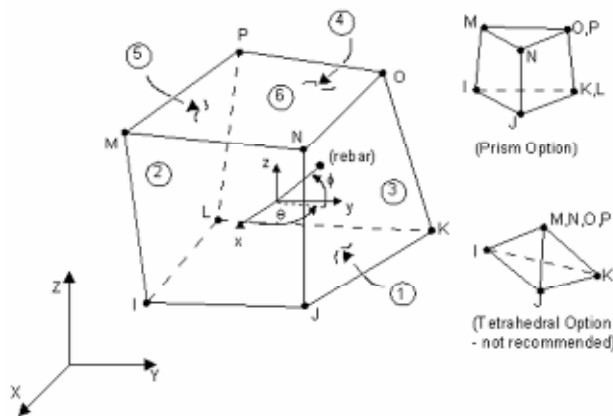


Figure (1): Brick element with 8 nodes (CONCRETE65 in ANSYS 16).

1-2 Finite Element Idealization of Reinforcement:

In this study the discrete model is used to represent steel reinforcement. The three-dimensional two-node bar element (**link8**) is a uniaxial tension-compression element with three degrees of freedom at each node (nodal translation in x, y and z) directions. The axial normal stress is assumed to be uniform over the entire element. The element x-axis is oriented along the length of the element from node (1) towards node (2) as shown in fig (2).

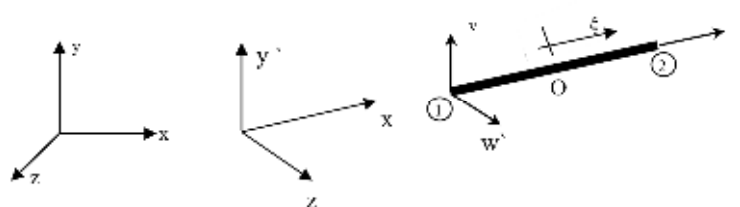


Figure (2): Bar element (LINK 8) in ANSYS 16

As the element is capable of carrying axial loads only, the strain-displacement relationship is as follows:

$$\epsilon = \epsilon_x = \frac{\partial u'}{\partial x'} \quad \text{-----} \quad (1)$$

Where: U' local displacement, X' local coordinate.

Concrete Modeling:

➤ **Stress-Strain Relationship:**

The Concrete 65 element requires linear isotropic and multilinear isotropic material properties to properly model concrete as shown in Fig.(3). The modulus of elasticity was calculated by eq. (2) taken from **ACI- code (2008)**.

$$E_c = 4730\sqrt{f'_c} \quad \text{-----} \quad (2)$$

The **ANSYS** program requires the uniaxial stress-strain relationship for concrete in compression as shown in fig. (5). Numerical expressions, eq. (3) and (4), were used along with eq. (5) to construct the uniaxial compressive stress-strain curve for concrete in this study **Cervenka, et al., (1997)**.

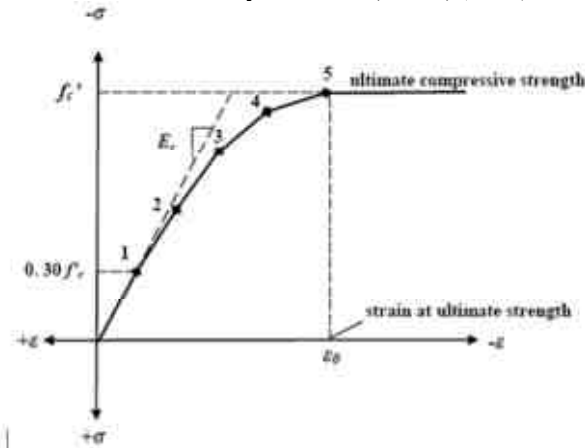


Figure (3): Simplified compressive uniaxial stress-strain curve for concrete Kachlakev et al. (2001).

$$f = \frac{E_c \varepsilon}{1 + \left(\frac{\varepsilon}{\varepsilon_0}\right)^2} \quad \text{-----} \quad (3)$$

$$\varepsilon_0 = \frac{2f'c}{E_c} \quad \text{-----} \quad (4)$$

$$E_c = \frac{f}{\varepsilon} \quad \text{-----} \quad (5)$$

Where: f = Stress at any strain ε .
 ε = Strain at stress f .
 ε_0 = Strain at the ultimate compressive strength $f'c$.

➤ **Cracking Modeling:**

In the finite element analysis of concrete structures, three different approaches have been employed for cracking modeling, **ANSYS 16.0 (2015)**.

- 1) Smearred- cracking model.
- 2) Discrete-cracking model.
- 3) Fracture-mechanism model.

In the present study is considered through an adjustment of material properties which effectively treats the cracking as a smeared band of cracks with fixed crack orientation.

➤ **Modeling of Crushing:**

If the material at an integration point fails in uniaxial, biaxial, or triaxial compression, the material is assumed to crush at that point. Under this condition, material strength is assumed to have degraded to an extent such that the contribution to the stiffness of an element at the integration point in the equation can be ignored, **ANSYS 16.0**

Modeling of Reinforcement:

Typical stress-strain curves for steel reinforcement bars used in concrete construction are obtained from coupon tests of bars loaded monotonically in tension. For all practical purposes, steel exhibits the same stress-strain curve in compression as in tension. The steel stress-strain relation exhibits an initial linear elastic portion, a

yield plateau, a strain-hardening range in which stress again increases with strain and finally a range in which the stress drops off until fracture occurs. The extent of the yield plateau is a function of the tensile strength of steel, where, $E_w = 0.1E_s$ **Cervenka et al. (1990)**.

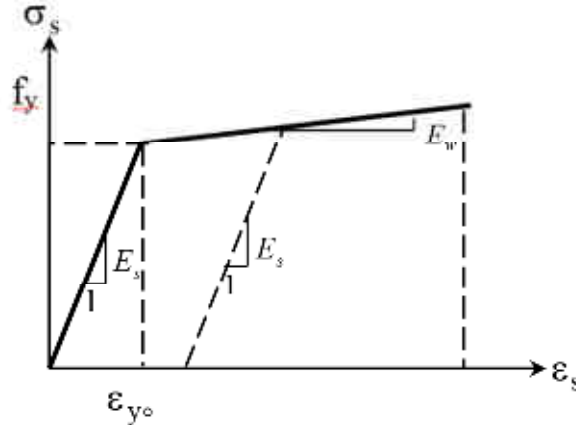


Figure (4): Typical stress-strain curve for steel bar, Mattock (1981)].

Nonlinear Solution Techniques

The nonlinear behavior of any reinforced concrete structure may be generally attributed to either material or geometric nonlinearity or a combination of both types. Only material nonlinearity is considered in the present study.

Full Newton-Raphson procedure:

The stiffness matrix is formed at every iteration. The advantage of this procedure may give more accurate results. The disadvantage of this procedure is that a large amount of computational effort may be required to form and decompose the stiffness matrix.

Convergence Criterion:

The convergence criteria for non-linear structural problems can usually be classified as:

1. **Force criterion.**
2. **Displacement criterion.**
3. **Work done criterion.**

For force convergence, the norm of the residual forces at the end of each iteration is checked against the norm of the current applied forces as:

$$\| \{R\} \| = (\sum R_i^2)^{0.5} \leq T_n (\sum F_i^{a2})^{0.5} \dots\dots\dots (6)$$

Where $\{R\}$ is the residual vector:

$$\{R\} = \{F^a\} - \{F^{nr}\} \dots\dots\dots (7)$$

In this study, the tolerance T_n is taken equal to 0.1% up to the ultimate load for load control.

Numerical Example

Four RC arch beams of 280*150 mm outer cross-section with a hollow core of 150*50 mm and 3000 mm long were constructed for this study as shown in Fig 8. A summary of the specimen's details can be found in Table 2, along with the average concrete compressive strength of which are made. The main reinforcement was 2Ø16mm. The stirrups were Ø5mm spaced at 60mm centers along the beams.

The test setup is shown in Fig 9. One end of the specimen was hinged by a steel roller to an anchored base to eliminate any horizontal movement. On the other end, the specimen was supported by a roller which allows the horizontal movement to occur. The load was applied as two point as shown in Fig 9 by 670 kN capacity hydraulic actuator.

Table (2): Summary of specimen details and concrete core compressive strength

Beam	Layout scheme/ section type	Concrete core compressive strength (MPa)	Splitting tensile strength (ft) (MPa)(**)
Arch Beam A1	Control beam (solid)	40.7	4.07
Arch beam A90	Arch beam with rectangular opening at 90°	39.4	3.9
Arch Beam A45	Arch beam with rectangular opening at 45°	39.06	3.9
Arch Beam A15	Arch beam with rectangular opening at 15°	43.06	4.3

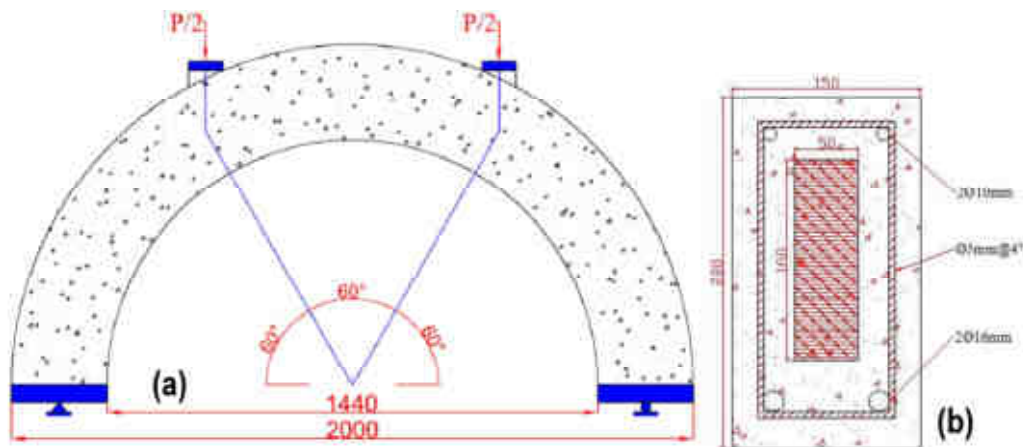


Figure (5); Geometry and Reinforcement Details of the Tested Specimens
 (a) Typical shape of a concrete arch beam specimen
 (b) Typical cross-section of arch hollow-box specimen beams .



Figure (6): Photo of test setup.

Finite Element Idealization:

The load was represented in the finite element model by 13 equivalent nodal forces across the width of the beam, as shown in Fig 10.

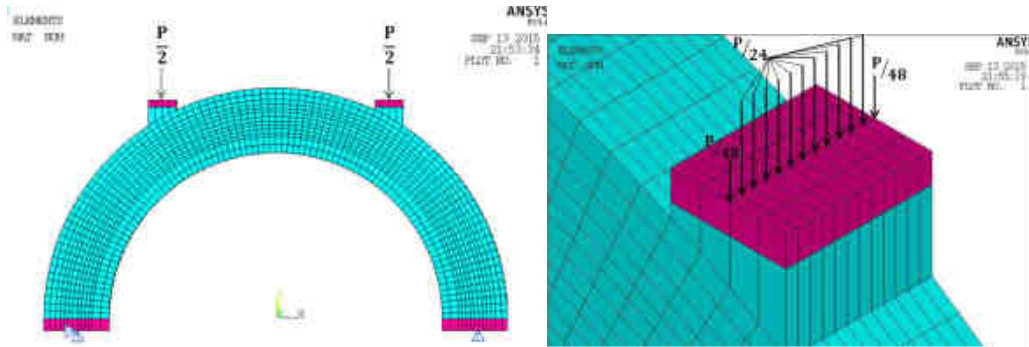


Figure (7): Finite elements mesh and load simulation for beams used in ANSYS program.

Results of the finite element model:

Figures (8 to 15) show the relationship between the experimental and numerical load-deflection and load-horizontal displacement of the beams, for both the experimental tests and the numerical analysis. The analytical results are detected quite well compared with that experimentally observed for beams.

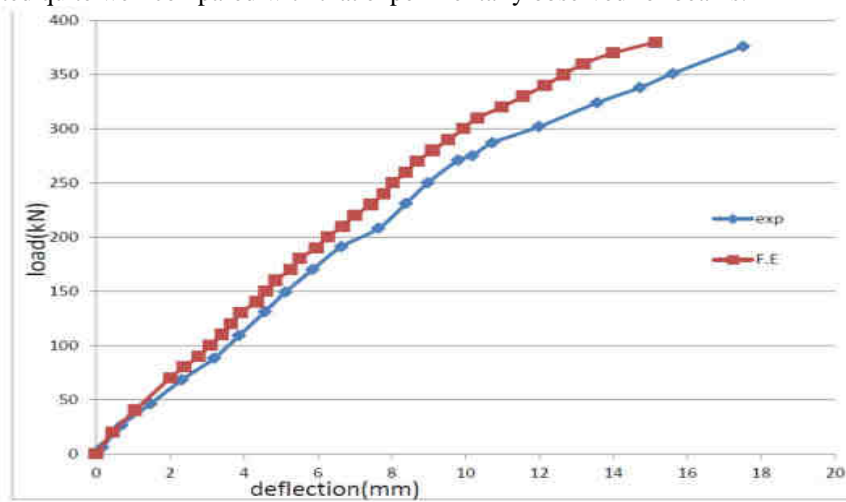


Figure (8): experimental and numerical load-deflection results of beam A1

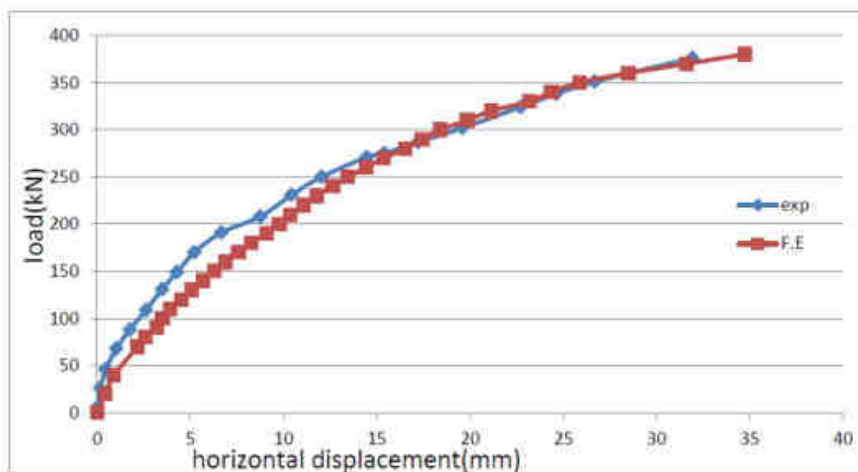


Figure (9): experimental and numerical load-horizontal displacement results of beam A1

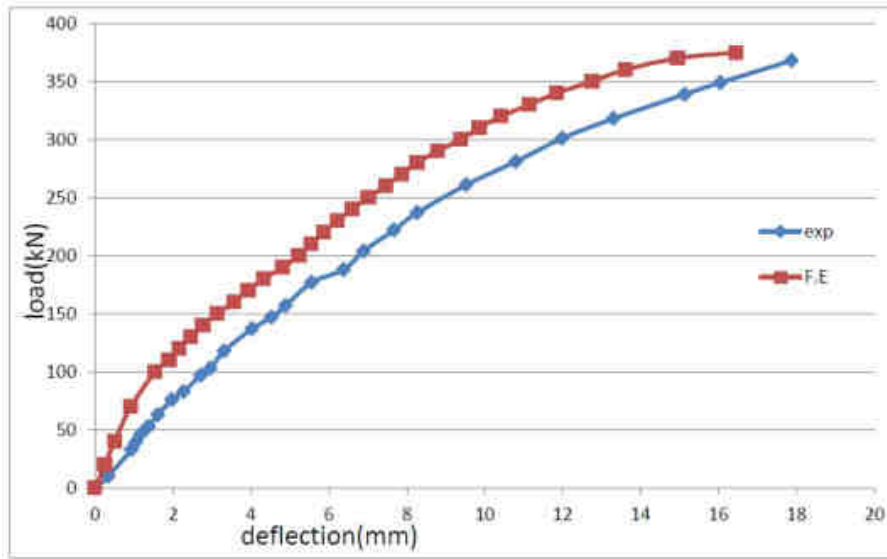


Figure (10): experimental and numerical load-deflection results of beam A90

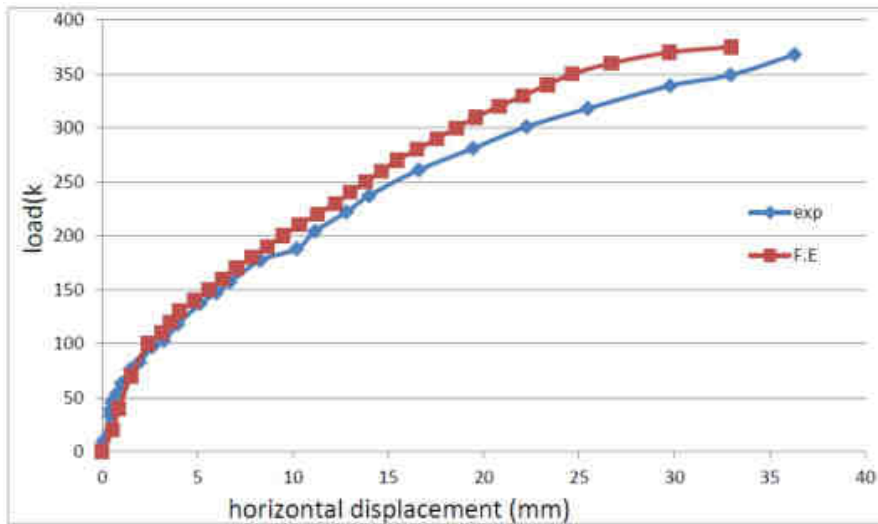


Figure (11): experimental and numerical load-horizontal displacement results of beam A90

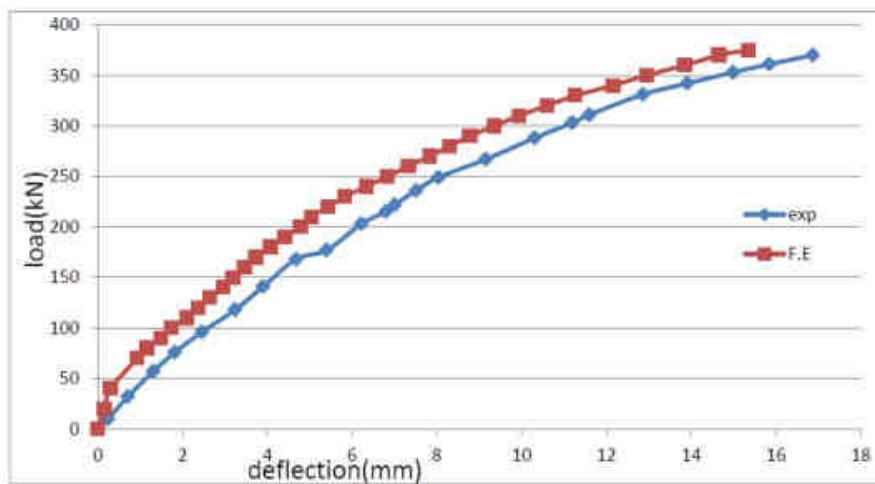


Figure (12): experimental and numerical load-deflection results of beam A15

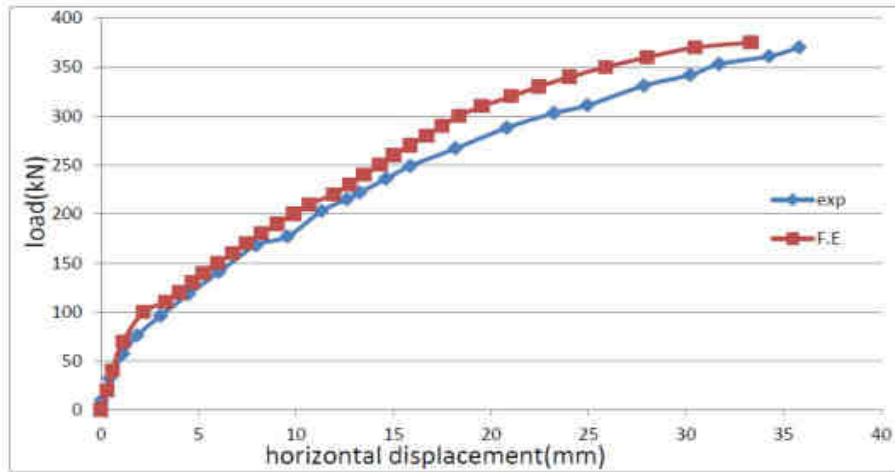


Figure (13): experimental and numerical load-horizontal displacement results of beam A15

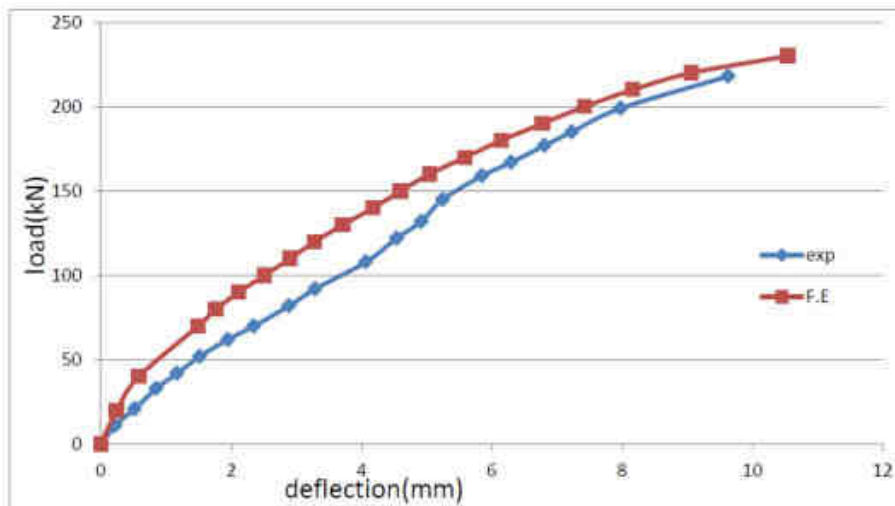


Figure (14): experimental and numerical load-deflection results of beam A45

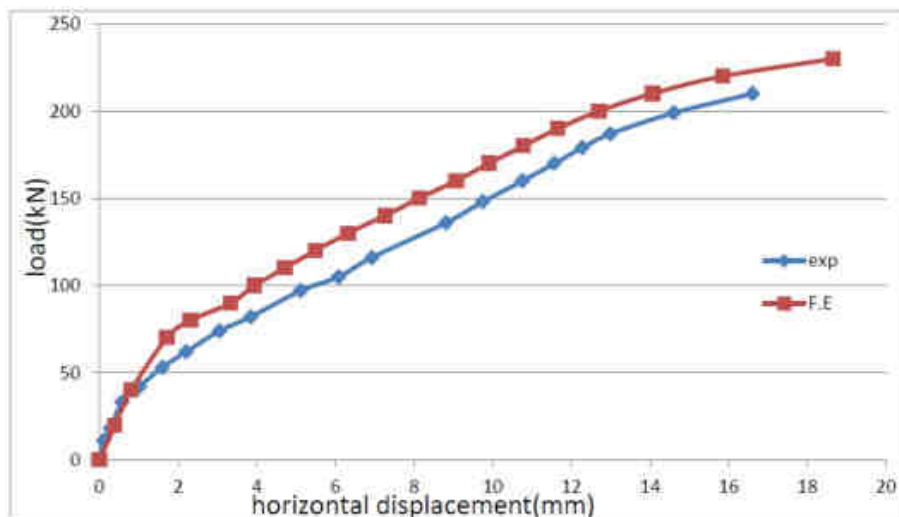


Figure (15): experimental and numerical load-horizontal displacement results of beam A45
Effect of opening location

To study the influence of opening location on the efficiency of RC arch hollow box beams, different locations were considered. Fig15 show the experimental and numerical strength capacity of arch beams according to the opening location.

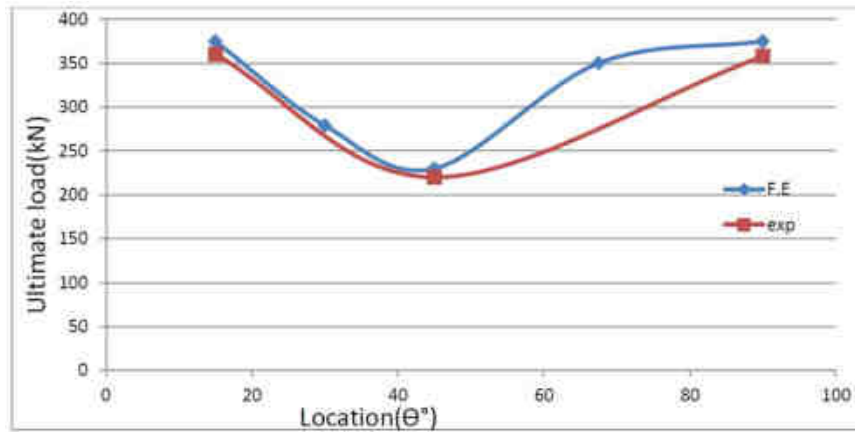
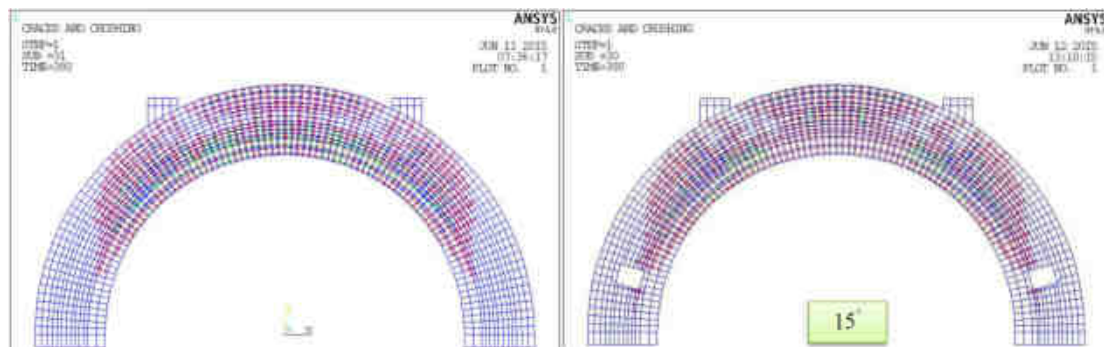


Figure (16) location-ultimate load carrying capacity

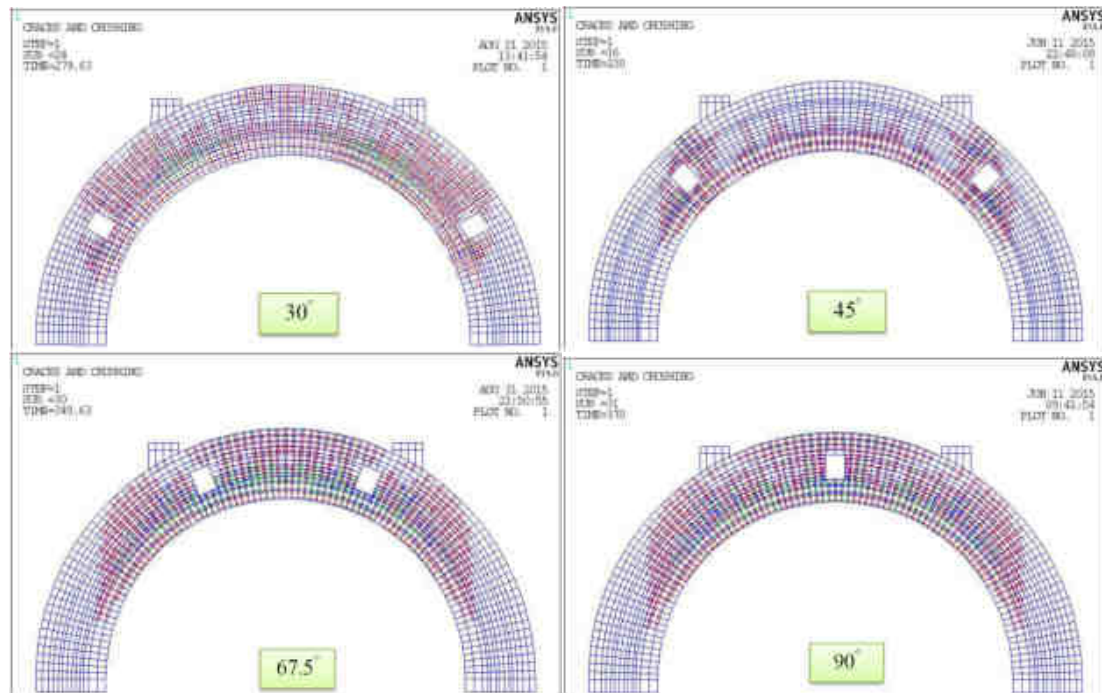
Table 3 illustrate the collapse loads obtained from this study together with the experimental values

Table 3: ultimate load for opening location condition study

specimen	Location (θ°)	Num. ultimate Load(kN)	Exp. ultimate Load(kN)
A15	15°	380	360
A30	30°	279	-----
A45	45°	230	220
A67.5	67.5°	350	-----
A90	90°	370	358



Figure(17)shows the crack pattern of beams A15, A30, A45, A67.5 and A90



Figure(17) continued

Conclusions

- 1-The three-dimensional nonlinear finite element model presented in this study by using the computer program (ANSYS V.16.0) is able to simulate the analysis of the arch hollow box RC beams. The numerical results were in good agreement with experimental load-deflection curves throughout the entire range of behavior.
- 2- The test results confirm that changing the location of the opening from 15° to 30° and 15 to 45° decrease the ultimate capacity of RC beams by 26% and 39% respectively.
- 3- Results confirm that changing the location of the opening from 45° to 67.5° and 45° to 90° increase the ultimate capacity of the RC beams by 52% and 60% respectively.

References:

- "ANSYS Manual", Version 16.0, U.S.A., 2004.
- American Concrete Institute, ACI Committee 318, (2008), "*Building Code Requirements for Structural Concrete (ACI 318-08) and Commentary (ACI 318R-08)*", American Concrete Institute, Farmington Hills, MI.
- Crisfield, M. A., (1979) "Iterative Solution Procedures for Linear and Nonlinear Structural Analysis" TRRL. Report LR900, Transport and Road Research Laboratory, Crowthome, England. Cited by (Zainul-Abideen, A.Y.A.).
- Cervenka, V., Eligehausen, R. and Pulkl, R., "*Sbeta-Computer Program for Nonlinear Finite Element Analysis of Reinforced Concrete Structures*", Report 90/1, Institute of Building Materials, University of Stulgort, 1990.
- Kachlakev Damian and Thomas Miller, "*Finite element modeling of reinforced concrete structures strengthened with FRP laminates*", Technical Report, Oregon Department of Transportation, pp.99, May (2001).
- Mansur, M.A., (2006). "Design of Reinforced Concrete Beams with Web Openings". Proceedings of the 6th Asia-Pacific Structural Engineering and Construction Conference (APSEC 2006), 5-6 September, Kuala Lumpur, Malaysia, pp.104-120.
- Mansur, M.A., (1998), "Effect of Openings on the Behavior and Strength of R/C Beams in Shear" *Cement and Concrete Composites* 20, pp.477-486.
- Mattock, A., "*Cyclic Shear Transfer and Type of Interface*", Journal of Structural Division, ASCE, Vol.107, N0.ST10, pp.1945-1964, October 1981.
- Nimmim, H. T., (1993), "Structural Behavior of Ferrocement Box-Beams" M.Sc., thesis, University of Technology.
- Zainul-Abideen, A.Y.A., (2010), "Experimental and Theoretical Investigation of Composite Steel-Concrete

Arches" Ph.D. Thesis, University of Technology, Iraq, 222pp.

Notation:

E_s	Modulus of Elasticity of Steel
f'_c	Uniaxial Compressive Strength of Concrete (Cylinder Test)
f_y	Yield strength of steel bar.
ε	Strain
σ	Stress